

Analysis of bubble breakup sensitivity on fluid properties using Large Eddy Simulations

Jan Kren^{1,2}, Blaž Mikuz¹

¹Reactor Engineering Division, Jožef Stefan Institute
Jamova cesta 39
1000 Ljubljana, Slovenia
jan.kren@ijs.si , blaz.mikuz@ijs.si

²Faculty of Mathematics and Physics, University of Ljubljana
Jadranska ulica 19
1000 Ljubljana, Slovenia

ABSTRACT

Two-phase flows play an important role in nuclear power systems during the boiling heat transfer or in the accident management conditions, e.g. during the evaporation of liquid water to steam caused by depressurization in loss of coolant accident (LOCA). An interesting phenomenon in two-phase flows is bubble breakup, which is a challenging process to model in the continuum approximation as the relevant physics takes place at the microscopic scales. Further investigations are needed to control and understand the physics of bubble breakup.

In this paper we present a sensitivity analysis of bubble breakup due to the fluid properties of gas-liquid mixture, such as viscosity and surface tension. We study this phenomenon in a vertical pipe with a diameter of 26 mm and the length of 520 mm. The study is focused on the slug flow regime, particularly a single Taylor bubble in counter-current turbulent flow. Taylor bubble is a long bullet-shaped gas bubble with a diameter almost matching that of the pipe.

The study is performed with Large Eddy Simulation approach in OpenFOAM computer code. We are using the modified interFoam Volume of Fluid (VoF) solver which enables the usage of higher order Runge-Kutta time-integration schemes integrated with PLIC interface reconstruction scheme. Turbulent sub-grid scales are modelled using the WALE model for eddy viscosity. This setup enables quantitative analysis of the impact of fluid properties on the rate of bubble breakup mechanism.

INTRODUCTION

In nuclear power systems, single and two-phase flows play an important role in maintaining safe operation of the nuclear power plants. Two-phase gas-liquid flow in a vertical pipe may appear in variety of patterns. Depending on basic flow parameters we can observe bubbly, slug, churn, annular or misty multiphase flow as can be seen in Figure 1. Our point of focus in this study is Taylor bubble flow, which is a sub-pattern of slug flow. Taylor bubble is a bullet-shaped bubble, which flows in a vertical pipe and occupies almost entire cross-section of the pipe.

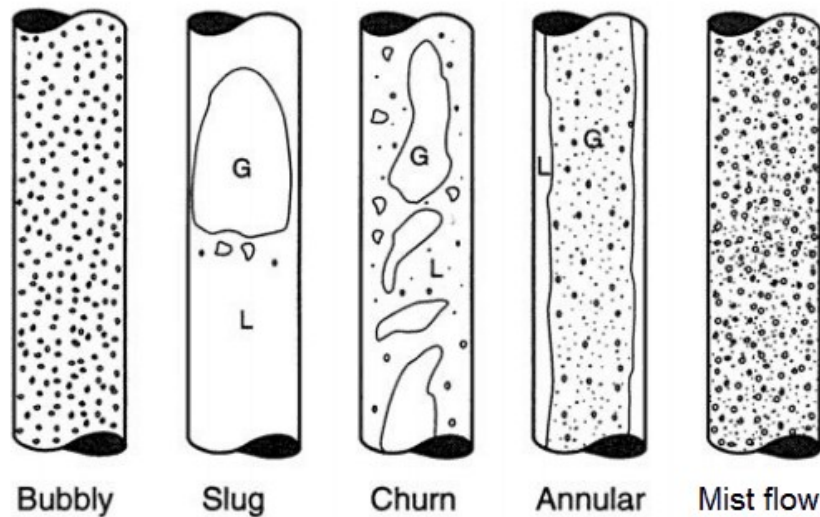


Figure 1: Two-phase flow regimes [1].

Experiments of the Taylor bubble addressed different settings and flow regimes. When the bubble is present in the background turbulent flow, the bubble's skirt exhibits chaotic flapping, which leads to the gradual breakup of the bubble. In order to measure that phenomenon for longer periods of time, counter-current turbulent flow has been proposed as a possible improvement in that regard and it turned out that the bubble stays trapped in the equilibrium position for hours and gradually decays. First experiments of the Taylor bubble in the counter-current turbulent flow were performed by Martin [2]. He demonstrated that the bubble velocity in the counter-current slug flow cannot be adequately represented by the existing theories for co-current background flow or stagnant liquid at that time.

In our studies, we are particularly interested in the physics of bubble breakup and coalescence and the development of the numerical models for the Large Eddy Method. Both topics are still in early stages of the development [3], [4]. First studies focused on the breakup in counter-current turbulent slug flow and re-coalescence in the bubble wake region were performed in a pipe with a diameter of 10 cm by Delfos et. al [5]–[7]. The bubble was held stationary in counter-current turbulent flow with a special spherical Teflon cap, which held the bubble at the exact position. This was possible as the point of interest in this study was the bubble wake region that is not affected by the placement of the spherical cap. Recent experiments of the Taylor bubble in the counter-current regime were performed with high-speed camera in visible light and a disintegration rate of the bubble has been measured [8], [9].

Shape and behaviour of a Taylor bubble depends on properties of the gas-liquid mixture. A comprehensive study of flow properties impact on Taylor bubble shape and behaviour in laminar conditions has been performed by Araujo [10]. They have performed two-dimensional numerical simulations of individual Taylor bubbles rising in vertical pipes filled with stagnant Newtonian liquid in laminar flow regime. A classification of the hydrodynamic properties of the bubble wake, liquid film and nose region has been performed based on the simulations, which covered wide ranges of dimensionless numbers such as Morton, Eötvös and Froude, namely

- $Eo = g(\rho_L - \rho_G)D^2/\sigma$; Eötvös number represents the ratio of surface tension and gravitational effects,
- $M = g\mu_L^4(\rho_L - \rho_G)/\rho_L^2\sigma^3$; Morton number contains the fluid properties only,

- $Fr = U_{TB}/\sqrt{gD(\rho_L - \rho_G)/\rho_L}$; Froude number defines the ratio of inertial and gravitational forces.

Current work focuses on the impact of flow and fluid properties of the water-air mixture on the gas loss of the main Taylor bubble. The numerical simulations have been performed with the open source computer code OpenFOAM. We are particularly interested in the effect of system temperature on the bubble breakup rate in the water-gas slug flow. Taylor bubble decay rate is being examined also experimentally at different flow conditions in the THELMA laboratory of the Reactor engineering division, Jožef Stefan Institute. The simulation results enable sensitivity analysis as well as an additional insight into the Taylor bubble behaviour, in particular at conditions when a precise long-term (i.e. several hours) control is hard to achieve in the experimental measurements.

THEORETICAL AND NUMERICAL BACKGROUND

A two-phase mixture of gas and liquid is modeled using the one-fluid formulation of the Navier-Stokes equations with the Volume-Of-Fluid (VOF) approach for interface capturing. In this method a void fraction α is introduced and the advection equation for this quantity is the following:

$$\partial_t \alpha + u \cdot \nabla \alpha = 0$$

with partial time derivative ∂_t , velocity vector u and gradient operator ∇ . The fluid mixture is described by the incompressible Navier-Stokes equations, i.e. the mass conservation equation,

$$\nabla \cdot u = 0$$

and momentum conservation equation

$$\partial_t(\rho u) + \nabla \cdot (\rho u u) = -\nabla p + \rho g + \nabla \left(\mu_{eff} (\nabla u + (\nabla u)^T) \right) + \sigma \kappa \delta(n) n$$

with mass density ρ , pressure p , gravitational acceleration g , effective mixture viscosity μ_{eff} , interface curvature κ , interface normal unit vector n and interface Dirac delta function $\delta(n)$.

Viscosity at the interface was calculated with harmonic averaging, namely:

$$1/\mu = \alpha_l/\mu_l + \alpha_g/\mu_g,$$

where α_l is the fraction of the liquid phase and α_g is fraction of the gas phase in the given computational cell, respectively. Similarly, μ_l and μ_g are the corresponding liquid and gas viscosities.

The described equations were solved in OpenFOAM v9 [11]. We have used a modified interFoam solver, which enables the usage of the Diagonally Implicit Runge-Kutta (DIRK) time integration schemes integrated with PLIC geometric reconstruction. This solver was based on a solver developed in OpenFOAM v4 by Frederix [12]. Turbulence at the sub-grid scales was modelled by the WALE model.

A recycling boundary condition was used at the inlet in order to achieve a fully developed turbulent flow. The flowrate was also adjusted at every timestep so that the net force on the bubble is always zero and the bubble stays at approximately constant position throughout the simulation.

Current work also focuses on the usage of the geometric VOF method, which is an improvement with respect to the algebraic VOF used in the previous versions of OpenFOAM and by Frederix [12]. Geometric VOF method can be divided into two steps – reconstruction and the advection of the interface [13]. The approximation of the interface is built from the information on the volume fraction. This can be done in various manners such as SLIC (Simple Line Interface Calculation) or PLIC (Piecewise-Linear Interface Calculation) interface reconstruction methods. In the next step, the reconstructed interface is advected by the given velocity field. Basic idea of these methods can be seen in Figure 2.

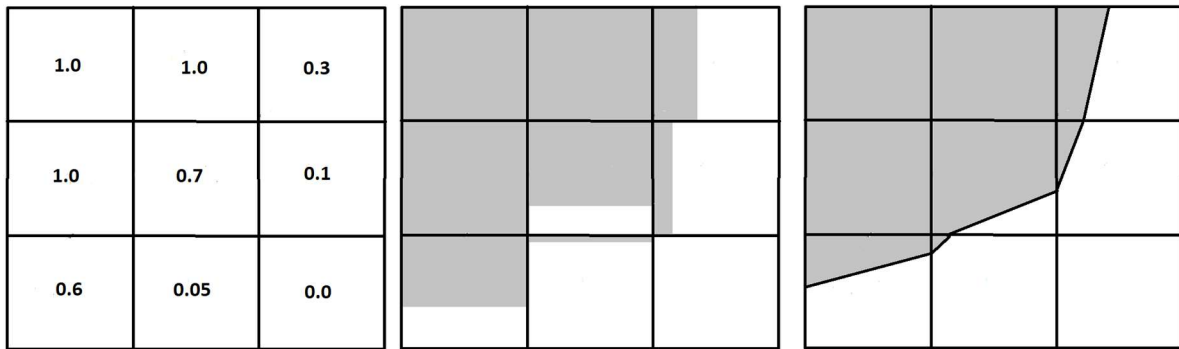


Figure 2: Reconstruction of the interface from the volume fractions (left) using SLIC (middle) or PLIC (right) method.

CASE SETUP

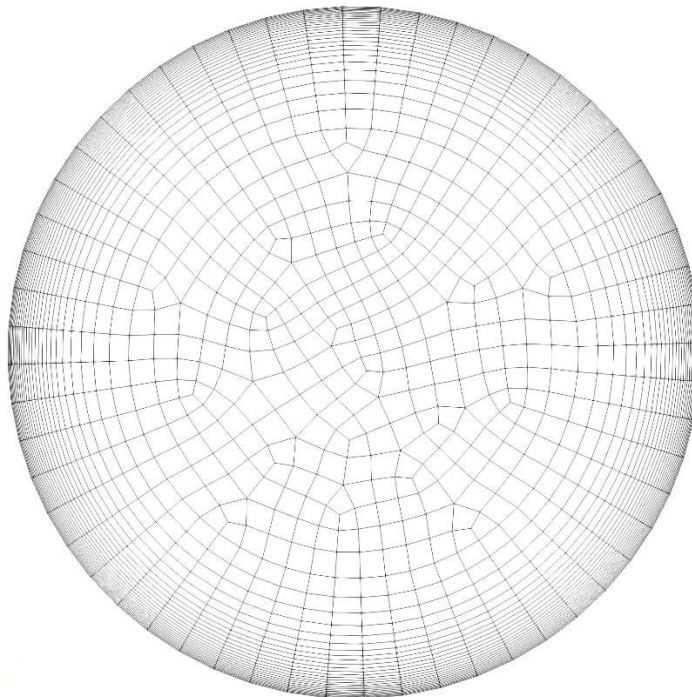


Figure 3: Cross-section of the numerical mesh.

In the present study, the fluid properties were selected to reproduce the water-air mixture. The pipe diameter was 26 mm and pipe length 52 cm. Numerical mesh with approximately 700000 cells was used with the fully hexahedral cells. The cross-section of the used mesh can be seen in Figure 3.

Current work focuses on the impact of temperature on the bubble breakup in the water-air mixture. We have prepared six simulations where the system temperature ranges from 283.15K (i.e. 10°C) to 372.15K (99°C) as can be seen in Table 1. The largest difference of a fluid property in this temperature range is observed in the kinematic viscosity of the water.

Table 1: Fluid properties for different cases [14].

Case	T [K]	ν_{water} [m^2/s]	ρ_{water} [kg/m^3]	ν_{air} [m^2/s]	ρ_{air} [kg/m^3]	σ [J/m^2]
1	283.15	1.31E-06	999.71	1.45E-05	1.1909	0.0742
2	293.15	1.01E-06	998.24	1.53E-05	1.1502	0.0727
3	313.15	6.60E-07	992.27	1.72E-05	1.0765	0.0696
4	323.15	5.55E-07	988.1	1.82E-05	1.0431	0.0679
5	333.15	4.75E-07	983.27	1.92E-05	1.0117	0.0662
6	372.15	2.97E-07	959.17	2.34E-05	0.90309	0.0589

Table 2: Morton, Froude, Eotvos and Reynolds numbers

Case	Mo	Fr	Eo	Re
1	7.096E-11	3.37E-01	89.22	3.37E+03
2	2.60E-11	3.37E-01	90.90	5.50E+03
3	5.38E-12	3.37E-01	94.44	6.70E+03
4	2.85E-12	3.37E-01	96.35	7.97E+03
5	1.63E-12	3.37E-01	98.34	9.30E+03
6	3.30E-13	3.37E-01	107.87	1.49E+04

From these properties we can derive the Morton, Eötvös, Froude and Reynolds number for each case. As can be seen from Table 2, the largest difference between these numbers can be seen in the Morton as well as Reynolds number. Froude and Eötvös numbers stay relatively the same. According to Araujo [10] it is clear that in this range of Morton, Froude and Eötvös number concave tail with wake is expected.

RESULTS

The main point of interest in this study is the bubble breakup at the Taylor bubbles skirt as can be seen at the left side of Figure 4. The bubble is exposed to the counter-current turbulent flow. In the film region the velocity of the liquid increases and induces instabilities at the air-water interface which causes the bubble breakup at the skirt of the bubble. This breakup can be characterized as the shearing-off process as well as a consequence of the large deformations of the bubble skirt caused by the turbulent fluctuations in the background turbulent flow. The shearing-off mechanism is considered as a special case of viscous shear break-up for the bubbles larger than about 5mm [4]. A number of small bubbles are sheared off the larger bubble due to the velocity profile in the gas and liquid phase.

Small bubbles that broke off can be reunited with the main bubble during the re-coalescence process, where the velocity field in the bubble wake region pushes small bubbles back into the main bubble. This process is not so pronounced in the current state of the numerical simulations as the additional coalescence models would be needed to correctly capture the re-coalescence process.

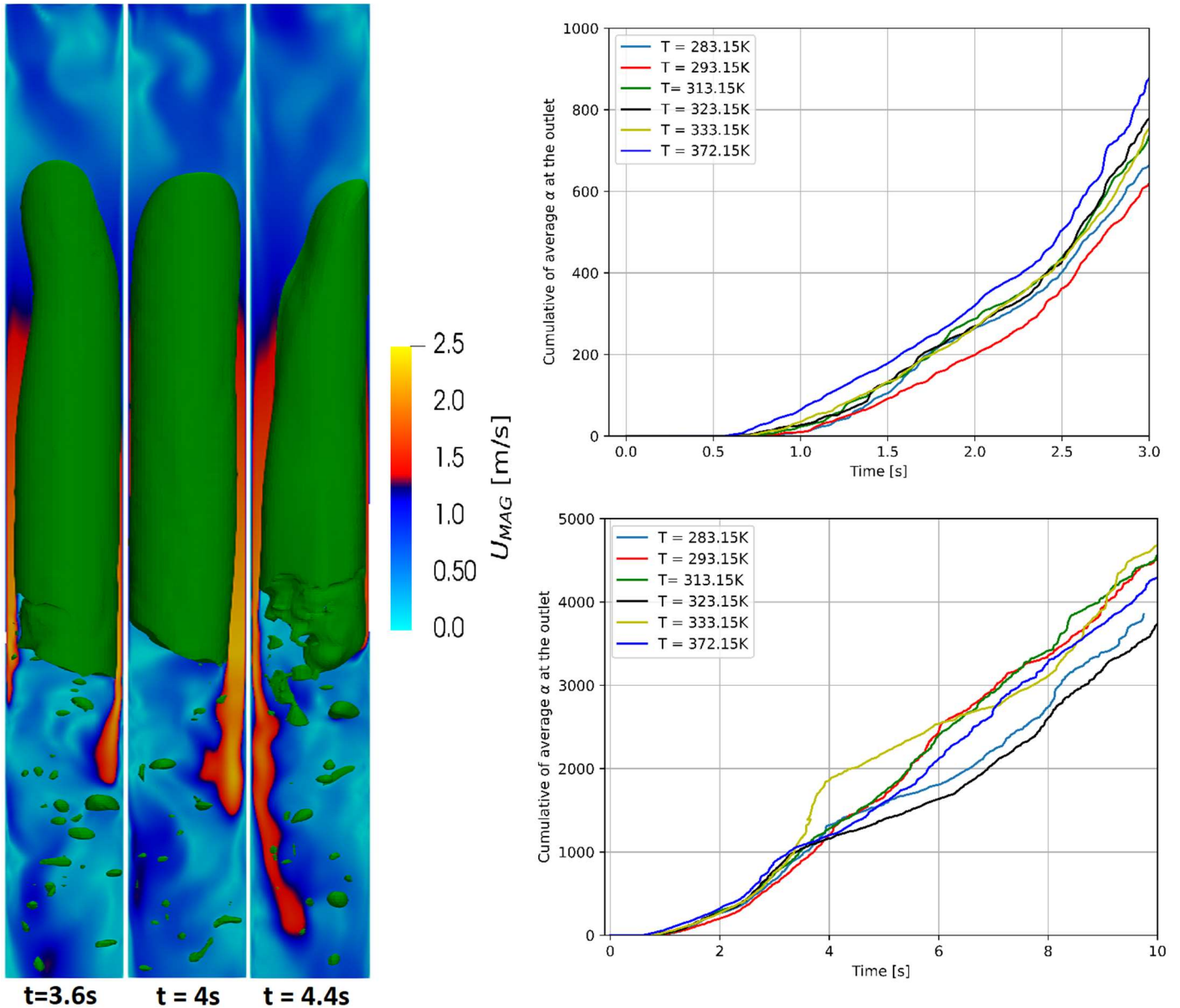


Figure 4: Instantaneous snapshots of Taylor bubble in counter-current flow (left), cumulative average void fraction at the outlet for first 3 seconds (top right) and for 10 seconds of simulations (bottom right)

Right side graphs in Figure 4 show the cumulative gas loss computed at the outlet of the computational domain. Firstly, we have simulated cases with different settings for 3 seconds. In this interval clear trend on the temperature is observed as can be seen in top right graph in Figure 4. The largest gas loss is observed at the highest temperature and then with some statistical uncertainties this gas loss decreases with temperature. We have extended the initial simulations for further 7 seconds. Bottom right graph in Figure 4 shows cumulative gas loss for the 10 seconds simulations. Clearly, after the initial 3 second period, the uniform dependence of the bubble decay rate on temperature is lost. This can be due to the number of reasons, i.e.:

1. The chaotic nature of the turbulence overrides the impact of the temperature in this range. Namely, the instantaneous eddies effectively break the expected trend. That could be improved with ensemble averaging of the results from several simulations starting from slightly different initial conditions.

2. Current simulations were calculated on the coarse mesh with 700k cells. Further study on the finer mesh is needed to eliminate the impact of the mesh on the results.
3. Our simulations applied Large eddy Simulation method with WALE model, which has been developed for single phase flows and is still underdeveloped for multiphase flows. Usage of more suited sub-grid scale model is needed in the future [3].

Figure 5 shows the void fraction at the outlet post-processed with a moving filter of 1 second width. We observe that the α increases in the first few seconds of the simulations and then fluctuates around a stable value. It is also visible that for the case 5 ($T = 333.15\text{K}$) there are two large bubbles that break off and significantly increases the α at the outlet. Thus, ensemble averaging will be needed in the future for statistically significant data. Differences based on fluid properties are again not observed.

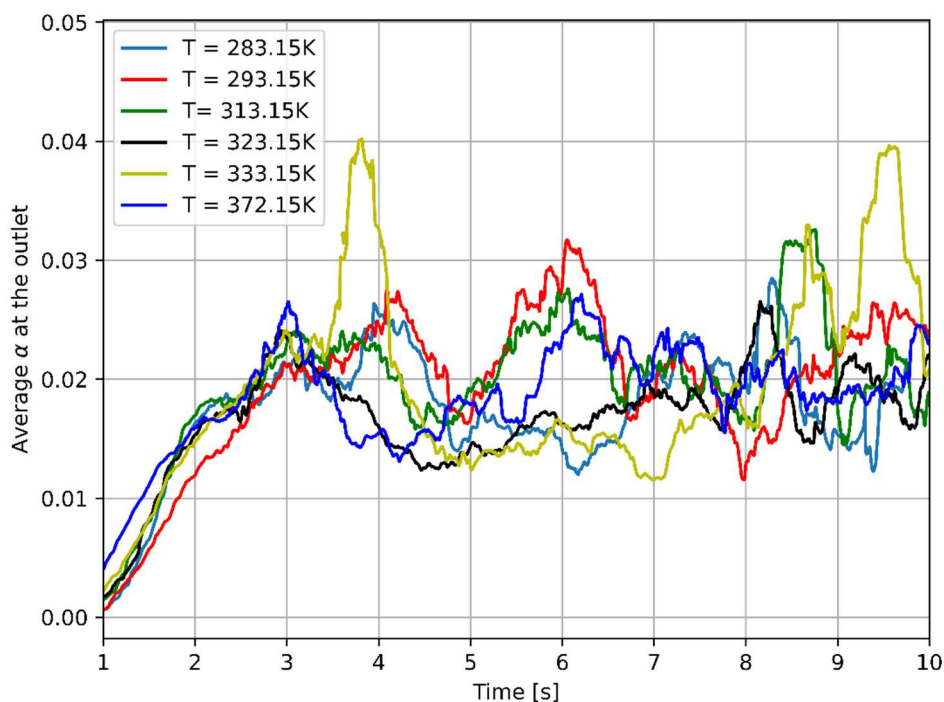


Figure 5: Void fraction at the outlet with added moving filter of 1s width.

CONCLUSIONS

In this paper we have presented analysis of bubble breakup sensitivity on water and air density, viscosity and surface tension in temperature range between 10°C and 99°C using Large Eddy Simulations with geometric VOF for interface capturing. For water-air mixture the bubble breakup does not show significant influence on the temperature. This can be due to the number of reasons, spanning from the too coarse numerical mesh, insufficient sub-grid scale models, which do not consider interface effects, and the stochastic nature of the turbulent flow, which requires ensemble averaging of the tests. For example, for the case 5 ($T = 333.15\text{K}$) one turbulent eddy significantly broke down the bubble and the expected pattern. Further evaluation of this work is needed in the future as well as experimental validation of the results. In computational aspect the results can be improved with the ensemble averaging of the multiple

simulations starting from slightly different initial conditions. Moreover, further validation of the code is needed on more benchmark test cases, such as Zalesak disc problem.

ACKNOWLEDGMENTS

The authors gratefully acknowledge financial support provided by Slovenian Research Agency, grant for Young Researcher Jan Kren.

REFERENCES

- [1] N. P. Cheremisinoff and R. Gupta, Eds., *Handbook of fluids in motion*. Ann Arbor, Mich: Ann Arbor Science, 1983.
- [2] C. S. Martin, “Vertically Downward Two-Phase Slug Flow,” *J. Fluids Eng.*, vol. 98, no. 4, pp. 715–722, Dec. 1976, doi: 10.1115/1.3448466.
- [3] M. Klein, S. Ketterl, and J. Hasslberger, “Large eddy simulation of multiphase flows using the volume of fluid method: Part 1—Governing equations and a priori analysis,” *Exp. Comput. Multiph. Flow*, vol. 1, no. 2, pp. 130–144, Jun. 2019, doi: 10.1007/s42757-019-0019-9.
- [4] Y. Liao and D. Lucas, “A literature review of theoretical models for drop and bubble breakup in turbulent dispersions,” *Chem. Eng. Sci.*, vol. 64, no. 15, pp. 3389–3406, Aug. 2009, doi: 10.1016/j.ces.2009.04.026.
- [5] R. Delfos, C. M. Rops, J. P. Kockx, and F. T. M. Nieuwstadt, “Measurement of the re-coalescence flux into the rear of a Taylor bubble,” *Phys. Fluids*, vol. 13, no. 5, pp. 1141–1150, May 2001, doi: 10.1063/1.1360713.
- [6] R. Delfos, C. J. Wisse, and R. V. A. Oliemans, “Measurement of air-entrainment from a stationary Taylor bubble in a vertical tube,” *Int. J. Multiph. Flow*, vol. 27, no. 10, pp. 1769–1787, Oct. 2001, doi: 10.1016/S0301-9322(01)00029-5.
- [7] J. P. Kockx, F. T. M. Nieuwstadt, R. V. A. Oliemans, and R. Delfos, “Gas entrainment by a liquid film falling around a stationary Taylor bubble in a vertical tube,” *Int. J. Multiph. Flow*, vol. 31, no. 1, pp. 1–24, Jan. 2005, doi: 10.1016/j.ijmultiphaseflow.2004.08.005.
- [8] Benattalah, Aloui, and Souhar, “Experimental Analysis on the Counter-Current Dumitrescu- Taylor Bubble Flow in a Smooth Vertical Conduct of Small Diameter,” *J. Appl. Fluid Mech.*, vol. 4, no. 04, Oct. 2011, doi: 10.36884/jafm.4.04.11940.
- [9] B. Mikuž, J. Kamnikar, J. Prošek, and I. Tiselj, “Experimental Observation of Taylor Bubble Disintegration in Turbulent Flow,” *Proc. 28th Int. Conf. Nucl. Energy New Eur.*, p. 9, 2019.
- [10] J. D. P. Araújo, J. M. Miranda, A. M. F. R. Pinto, and J. B. L. M. Campos, “Wide-ranging survey on the laminar flow of individual Taylor bubbles rising through stagnant Newtonian liquids,” *Int. J. Multiph. Flow*, vol. 43, pp. 131–148, Jul. 2012, doi: 10.1016/j.ijmultiphaseflow.2012.03.007.
- [11] The OpenFOAM Foundation, “OpenFOAM | Free CFD Software,” 2022. <https://openfoam.org/> (accessed Jan. 05, 2022).
- [12] E. M. A. Frederix, E. M. J. Komen, I. Tiselj, and B. Mikuž, “LES of Turbulent Co-current Taylor Bubble Flow,” *Flow Turbul. Combust.*, vol. 105, no. 2, pp. 471–495, Aug. 2020, doi: 10.1007/s10494-020-00118-0.
- [13] D. Dai and A. Y. Tong, “Analytical interface reconstruction algorithms in the PLIC-VOF method for 3D polyhedral unstructured meshes,” *Int. J. Numer. Methods Fluids*, vol. 91, no. 5, pp. 213–227, Oct. 2019, doi: 10.1002/flid.4750.
- [14] D. Siderius, “NIST Standard Reference Simulation Website - SRD 173.” National Institute of Standards and Technology, Sep. 01, 2017. doi: 10.18434/T4M88Q.